782 cm^{-1} (v s, $\nu_{as}(Os^{18}O_2)$).

Os(η^4-CHBA-DCB)(PPh_3)$_2$ (11). To a 50-mL Erlenmeyer flask with a stir bar were added $K_2[Os(\eta^4\text{-CHBA-DCB})(O)_2]$ (**10**) (221 mg, 0.260 mmol), triphenylphosphine (450 mg), ca. 5 mL of trifluoroacetic acid, and 10 mL of THF. The orange solution was heated until most of the THF had evaporated and a dark green molten triphenylphosphine mixture remained (ca. 10 min). After cooling, the mixture was dissolved in 10 mL of CH_2Cl_2 and the solution was placed on a short silica gel column. Elution with CH_2Cl_2 removed the product as a green band. Addition of hexane followed by removal of CH_2Cl_2 yielded the product as a dark green crystalline solid: yield 236 mg (72%); ^1H NMR (Table I). Anal. Calcd for $C_{56}H_{36}Cl_6N_2O_4OsP_2$: C, 53.14; H, 2.87; N, 2.21. Found: C, 53.33; H, 2.94; N, 2.22.

Os(η^4-CHBA-DCB)(*t*-Bupy)(PPh_3) (12). Os(η^4-CHBA-DCB)(PPh_3)$_2$ (**11**) (75 mg, 0.0593 mmol) was dissolved in 50 mL of CH_2Cl_2. Addition of 4-*tert*-butylpyridine followed by heating under reflux for 0.5 h produced a color change from dark green to light blue. Removal of solvents followed by recrystallization from CH_2Cl_2/hexane yielded the product as a dark blue crystalline solid. NMR showed the presence of 0.5 molecule of hexane per molecule of complex: yield 58 mg (86%); ^1H NMR (Table I). Anal. Calcd for $C_{47}H_{34}Cl_6N_3O_4OsP\cdot0.5(C_6H_{14})$: C, 50.82; H, 3.50; N, 3.56. Found: C, 50.72; H, 3.51; N, 3.53.

Os(η^4-CHBA-DCB)(*t*-Bupy)$_2$ (13). Os(η^4-CHBA-DCB)(PPh_3)$_2$ (**11**) (200 mg, 0.158 mmol) was dissolved in 20 mL of neat *t*-Bupy. The solution was heated under reflux for 15 min during which time the color changed from dark green to very dark blue, almost black. The *t*-Bupy was removed under vacuum and the crude product recrystallized from CH_2Cl_2/hexane. This yielded the pure product as a very dark crystalline solid. NMR showed the presence of 0.25 molecule of hexane per molecule of complex: yield 108 mg (68%); ^1H NMR (Table I). Anal. Calcd for $C_{38}H_{32}Cl_6N_4O_4Os\cdot0.25$ (C_6H_{14}): C, 45.92; H, 3.46; N, 5.42. Found: C, 46.20; H, 3.52; N, 5.37.

Os(η^4-CHBA-DCB)(*t*-BuNC)$_2$ (14). $K_2[Os(\eta^4\text{-CHBA-DCB})(O_2)]$ (**10**) (120 mg, 0.135 mmol), triphenylphosphine (90 mg, 2.5 equiv), and *tert*-butyl isocyanide (0.20 mL, 12 equiv) were dissolved in 10 mL of THF and heated under reflux for 1.25 h. The solution was evaporated to dryness and the orange residue dissolved in CH_2Cl_2 and transferred to the top of a short silica gel column. The phosphine was removed by eluting with 300 mL of CH_2Cl_2, and the bright orange Os(III) intermediate was then removed with THF/acetone (1:1). This solution was concentrated and then treated with a dilute Br_2/THF solution at room temperature. The oxidation to the blue Os(IV) product was followed by TLC, and upon completion the reaction mixture was evaporated to dryness. The crude product was dissolved in 5 mL of CH_2Cl_2 and passed down a short silica gel column with CH_2Cl_2. Addition of hexane followed by removal of CH_2Cl_2 yielded the product as a dark blue crystalline solid: yield 20 mg (16%); ^1H NMR (Table I). Anal. Calcd for $C_{30}H_{24}Cl_6N_4O_4Os$: C, 39.71; H, 2.67; N, 6.17. Found: C, 39.75; H, 2.70; N, 6.19.

Os(η^4-CHBA-DCB)(bpy) (15). Os(η^4-CHBA-DCB)(PPh_3)$_2$ (**11**) (120 mg, 0.095 mmol) and bipyridine (210 mg, 1.34 mmol) were dissolved in toluene (10 mL) and heated under reflux for 0.5 h during which time the color darkened. The cooled solution was placed on a short silica gel column and eluted with excess CH_2Cl_2 to separate the product from starting material and 62 mg (78%) of product was isolated and recrystallized from CH_2Cl_2/hexane. Crystals for X-ray analysis were grown by vapor diffusion employing CH_2Cl_2/EtOH.

Acknowledgment. We acknowledge the donors of the Petroleum Research Fund, administered by the American Chemical Society, the Research Corporation, the Atlantic Richfield Corporation of America, and Occidental Research Inc. for support to T.J.C. and the National Science Foundation (Grant CHE-8107535 to T.J.C. and CHE 78-08716 to F.C.A.). S.L.G. is an NSF Predoctoral Fellow and T.E.K. is the Caltech Union Carbide Fellow in Chemical Catalysis. We thank John McNally for assistance with ligand preparations, Drs. William P. Schaefer and Richard E. Marsh for helpful discussions, and Engelhard Corporation for a generous donation of precious metal compounds. Operation of the Bruker WM-500 NMR spectrometer at the Southern California Regional NMR facility was supported by National Science Foundation Grant CHE-7916324.

Registry No. 1, 90791-62-1; **2**, 90791-63-2; **3**, 90791-45-0; **4**, 90791-46-1; **5** (L = py), 90791-47-2; **5** (L = *t*-Bupy), 90791-53-0; **7** (L = py), 90791-48-3; **7** (L = *t*-Bupy), 90791-54-1; **8a**, 90791-49-4; **8b**, 90791-50-7; **8***, 90791-51-8; **9** (L = py), 90865-92-2; **9** (L = *t*-Bupy), 90791-55-2; **9′** (L = py), 90791-52-9; **9′** (L = *t*-Bupy), 90865-47-7; **10**, 90791-56-3; **11**, 90791-57-4; **12**, 90791-58-5; **13**, 90791-59-6; **14**, 90791-60-9; **15**, 90791-61-0; TFA, 76-05-1; TBAP, 1923-70-2; H_4CHBA-ethylene, 90791-64-3; H_4CHBA-*t*-1,2-diMeO-Et, 90791-65-4; H_4CHBA-*t*-1,2-diEtO-Et, 90791-66-5; $K_2[Os(OH)_4(O)_2]$, 77347-87-6; $^{18}O_2$, 32767-18-3; 2-acetylsalicyclic acid, 50-78-2; ethylenediamine, 107-15-3; 3,5-dichloroacetylsalicylic acid, 54223-75-5; 4,5-dichloro-*o*-phenylenediamine, 5348-42-5; tetrabutylammonium periodate, 65201-77-6.

Supplementary Material Available: Tables of data collection information, atom coordinates, Gaussian amplitudes, bond lengths and angles, and a listing of structure factor amplitudes (144 pages). Ordering information is given on any current masthead page.

Electrochemistry and Spectroelectrochemistry of σ-Bonded Iron Aryl Porphyrins. 1. Evidence for Reversible Aryl Migration from Iron to Nitrogen of Five-Coordinate Complexes

D. Lançon,[1a] P. Cocolios,[1a] R. Guilard,[1b] and K. M. Kadish*[1a]

Contribution from the Department of Chemistry, University of Houston, Houston, Texas 77004, and the Laboratoire de Synthèse et d'Electrosynthèse Organométallique Associé au CNRS (LA 33), Faculté des Sciences "Gabriel", 21100 Dijon, France. *Received January 4, 1984*

Abstract: The iron aryl σ-bonded porphyrins (OEP)Fe(C_6H_5) and (TPP)Fe(C_6H_5) were studied by electrochemical and spectroelectrochemical techniques. Under appropriate conditions both complexes undergo one reversible single-electron reduction and two reversible single-electron oxidations. However, at slow scan rates the first oxidation process is followed by an irreversible chemical reaction producing a new electroactive species. This species may be further oxidized by one electron to yield the corresponding iron(III) *N*-phenyl derivative. The latter species is reversibly reduced by one electron to give $[(N\text{-}C_6H_5P)Fe^{II}]^+$, where P = OEP or TPP. This complex undergoes an overall two-electron irreversible reduction involving back-migration of the phenyl group from the nitrogen to the iron atom, thus generating the starting material in its reduced form.

During the past decade, studies of substrate activation by cytochrome P-450 have revealed the formation of σ-iron(III) alkyl (or aryl) P-450 complexes. Both in vivo experiments and use of model compounds have been carried out in order to elucidate the

0002-7863/84/1506-4472$01.50/0

pathways and mechanisms leading to formation of these unusual complexes during substrate activation.[2-14] More recently, it has been suggested that cytochrome P-450, myoglobin, and hemoglobin give rise to intermediate σ-iron(III) alkyl (aryl) derivatives upon metabolic oxidation of various monosubstituted hydrazines by these hemoproteins, the final products being the corresponding *N*-alkyl- or *N*-arylporphyrins.[15-16] These hypotheses have been tested in studies of methyl- and phenylhydrazine oxidation by synthetic iron porphyrins[17] as well as by studies on the oxidative migration of alkyl (aryl) groups from metal to nitrogen in synthetic iron porphyrins.[18,19]

Several early attempts to synthesize model iron porphyrin complexes containing a σ-alkyl- or σ-aryl-iron bond have been reported,[20-22] but it is only recently that these complexes have been fully characterized.[18,23-27] The σ bond introduces very unusual electronic and structural properties to the (P)Fe(R) complexes. For example, (P)Fe(R) (where R = alkyl or aryl group) are pentacoordinate low-spin iron(III) derivatives. In addition, electrochemical measurements[23-26] indicate dramatic cathodic shifts in half-wave potentials for both oxidation and reduction of the Fe(III) complexes. These shifts are up to 750 mV compared to oxidation/reduction of the corresponding (P)FeX derivatives in similar solvents.

Most previous electrochemical studies of σ-bonded metal porphyrins have concentrated on measuring redox potentials, and only one paper has reported the chemistry of the electrooxidized species.[28] In this paper we report the electrochemistry and spectroelectrochemistry of (OEP)Fe(C_6H_5) and (TPP)Fe(C_6H_5) in the nonbonding benzonitrile and describe the mechanism for a reversible electrochemically initiated, metal-to-nitrogen migration of the phenyl group yielding iron(III) *N*-phenylporphyrins. Characterization of this mechanism and identification of several novel species are by electrochemical and spectroelectrochemical techniques.

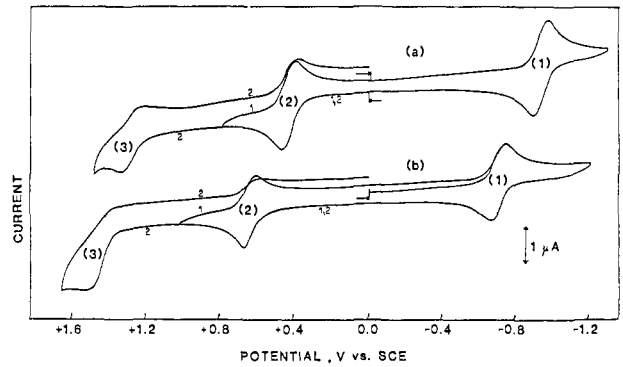

Figure 1. Cyclic voltammogram of (a) 1.0×10^{-3} M (OEP)Fe(C_6H_5) and (b) 0.9×10^{-3} M (TPP)Fe(C_6H_5) in PhCN, 0.1 M TBA(PF_6). Scan rate = 100 mV/s. Reactions 1, 2 and 3 are represented in the text.

Experimental Section

Instrumentation. Cyclic voltammetry experiments with scan rates lower than 500 mV/s were carried out with either a Princeton Applied Research Model 174A potentiostat, a BAS Model CV-1B, or an IBM Instruments Model EC225 voltammetric analyzer. Current–voltage curves were recorded on a Houston Instrument Model 2000 X-Y recorder. For scan rates higher than 500 mV/s, a PAR Model 174A potentiostat and 175 universal programmer or an IBM Instruments Model EC225 voltammetric analyzer were used. In this case the current–voltage traces were recorded on a Tektronix Model 5111 oscilloscope coupled with a Tektronix C5-A camera. A three-electrode system was used with a Pt button working electrode, a Pt wire counterelectrode, and a saturated calomel electrode (SCE) as reference. To minimize aqueous contamination, the reference electrode was separated from the bulk of the solution by a cracked-glass or fritted-glass bridge, filled with the solvent plus supporting electrolyte. The supporting electrolyte solutions were systematically deoxygenated by a solvent-saturated stream of nitrogen for at least 10 min before introduction of the porphyrin and were protected from air by a nitrogen blanket during the experiment.

Spectroelectrochemical experiments were performed at an optically transparent thin-layer electrode (OTTLE)[29] which consisted of a 1000 lpi (lines/in.) gold minigrid sandwiched between two glass slides, with a typical width of 0.10 mm. Potentials were monitored with a Bioanalytical Systems Model CV-1B or an IBM Instruments Model EC225 voltammetric analyzer. Scan rates were maintained below 3 mV/s. Because of high resistances inherent to the cell design, concentrations of supporting electrolyte were 0.3 M. A Tracor Northern Model 1710 holographic optical spectrometer multichannel analyzer was used for all UV–visible measurements. Spectra from 290 to 920 nm resulted from the signal averaging of a minimum of 50 sequential spectral acquisitions simultaneously recorded by a 512 diode array, providing a spectral resolution of 1.2 nm per diode. Wavelength calibration was achieved with a holmium oxide filter.

Materials. (P)Fe(C_6H_5), where P = OEP and TPP, was synthesized from (P)FeCl according to published procedures.[28] The purity of the complexes was checked by ^1H NMR, IR, and UV–visible spectroscopies. All solvents used for the electrochemical experiments were purchased as reagent grade quality. Benzonitrile (PhCN) was distilled from P_2O_5 under inert atmosphere while 1,2-dimethoxyethane (DME) was used as received. The supporting electrolyte, tetra-*n*-butylammonium hexafluorophosphate (TBA(PF_6)), purchased from Fluka Co., was recrystallized from EtOH, dried in vacuo at 100 °C, and stored in a desiccator.

Results and Discussion

Electrochemical and Spectroelectrochemical Measurements. Typical cyclic voltammograms of (OEP)Fe(C_6H_5) and (TPP)-Fe(C_6H_5) in PhCN, 0.1 M TBA(PF_6), are shown in Figure 1.

(1) (a) University of Houston. (b) Laboratoire de Synthèse et d'Electrosynthèse Organométallique Associé CNRS (LA 33).
(2) Uehleke, H.; Hellmer, K. H.; Ullrich, V. *Arch. Pharm. (Weinheim, Ger.)* **1973**, *279*, 39.
(3) Mansuy, D.; Nastainczyk, W.; Ullrich, V. *Arch. Pharm. (Weinheim, Ger.)* **1974**, *285*, 315.
(4) Wolf, C. R.; Mansuy, D.; Nastainczyk, W.; Deutschmann, G.; Ullrich, V. *Mol. Pharmacol.* **1977**, *13*, 315.
(5) Mansuy, D. *Pure Appl. Chem.* **1980**, *52*, 698.
(6) Mansuy, D.; Chottard, J. C.; Lange, M.; Battioni, J. P. *J. Mol. Catal* **1980**, *7*, 215.
(7) Mansuy, D.; Guerrin, P.; Chottard, J. C. *J. Organomet. Chem.* **1979**, *171*, 195.
(8) Guerrin, P.; Battioni, J. P.; Chottard, J. C.; Mansuy, D. *J. Organomet. Chem.* **1981**, *218*, 201.
(9) Brault, D.; Bizet, C.; Morliere, P.; Rougee, M.; Land, E. J.; Santus, R.; Shallow, A. J. *J. Am. Chem. Soc.* **1980**, *102*, 1015.
(10) Mansuy, D. *Rev. Biochem. Toxicol.* **1981**, *3*, 283.
(11) Brault, D.; Neta, P. *J. Am. Chem. Soc.* **1981**, *103*, 2705.
(12) Mansuy, D.; Fontecave, M.; Battioni, J. P. *J. Chem. Soc., Chem. Commun.* **1982**, 317.
(13) Mansuy, D.; Battioni, J. P. *J. Chem. Soc., Chem. Commun.* **1982**, 638.
(14) Brault, D.; Neta, P. *J. Phys. Chem.* **1982**, *86*, 3405.
(15) Augusto, O.; Kunze, K. L.; Ortiz de Montellano, P. R. *J. Biol. Chem.* **1982**, *257*, 6231.
(16) Ortiz de Montellano, P. R.; Kunze, K. L. *J. Am. Chem. Soc.* **1981**, *103*, 6534.
(17) Battioni, P.; Mahy, J. P.; Gillet, G.; Mansuy, D. *J. Am. Chem. Soc.* **1983**, *105*, 1399.
(18) Ortiz de Montellano, P. R.; Kunze, K. L.; Augusto, O. *J. Am. Chem. Soc.* **1982**, *104*, 3545.
(19) Mansuy, D.; Battioni, J. P.; Dupré, D.; Sartori, E.; Chottard, G. *J. Am. Chem. Soc.* **1982**, *104*, 6159.
(20) Clarke, D. A.; Grigg, R.; Johnson, A. W. *J. Chem. Soc., Chem. Commun.* **1966**, 208.
(21) Clarke, D. A.; Dolphin, D.; Grigg, R.; Johnson, A. W.; Pinnock, H. A. *J. Chem. Soc. C* **1968**, 881.
(22) Reed, C. A.; Mashiko, T.; Bentley, S. P.; Kastner, M. E.; Scheidt, W. R.; Spartalian, K.; Lang, G. *J. Am. Chem. Soc.* **1979**, *101*, 2948.
(23) Lexa, D.; Mispelter, J.; Saveant, J. M. *J. Am. Chem. Soc.* **1981**, *103*, 6806.
(24) Lexa, D.; Saveant, J. M. *J. Am. Chem. Soc.* **1982**, 104, 350.
(25) Lexa, D.; Saveant, J. M.; Battioni, J. P.; Lange, M.; Mansuy, D. *Angew. Chem., Int. Ed. Engl.* **1980**, *20*, 578.
(26) (a) Cocolios, P.; Laviron, E.; Guilard, R. *J. Organomet. Chem.* **1982**, *228*, C39. (b) Cocolios, P.; Lagrange, G.; Guilard, R. *J. Organomet. Chem.*, **1983**, *265*, 65.
(27) Ogoshi, H.; Sugimoto, H.; Yoshida, Z. I.; Kobayashi, H.; Sakai, H.; Maeda, Y. *J. Organomet. Chem.* **1982**, *234*, 185.
(28) Dolphin, D.; Halko, D. J.; Johnson, E. *Inorg. Chem.* **1981**, *20*, 4348.
(29) Rhodes, R. K.; Kadish, K. M. *Anal. Chem.* **1981**, *53*, 1539.

Table I. Maximum Absorbance Wavelengths (λ_{max}) and Corresponding Molar Absorptivities (ϵ) of Several σ-Bonded Iron Porphyrins in PhCN, 0.3 M TBA(PF_6)

species	λ_{max}, nm ($\epsilon \times 10^{-3}$)	
(OEP)Fe(C_6H_5)	393 (129)	527 (sh), 554 (22)
[(OEP)Fe(C_6H_5)]$^+$	392 (120)	530 (20), 555 (sh)
[(OEP)Fe(C_6H_5)]$^-$	350 (42), 408 (98)	502 (19), 542 (57), 758 (7)
(TPP)Fe(C_6H_5)	398 (sh), 412 (93)	522 (12), 541 (sh)
[(TPP)Fe(C_6H_5)]$^-$	364 (36), 429 (98)	510 (14), 533 (sh), 571 (4), 765 (4)
(C_{12}TPP)Fe(n-C_4H_9)[a]	391 (sh), 411 (130)	516 (14), 530 (sh)
[(C_{12}TPP)Fe(n-C_4H_9)]$^-$[a]	363 (50), 424 (85)	500 (19), 529 (sh), 611 (7), 714 (3)

[a] From ref 23. Spectra recorded in DMF, 0.1 M TBAP.

Both complexes exhibit one reduction (eq 1) and two oxidations (eq 2 and 3) within the potential range of the solvent. The

$$(P)Fe(C_6H_5) + e^- \rightleftarrows [(P)Fe(C_6H_5)]^- \quad (1)$$

$$(P)Fe(C_6H_5) \rightleftarrows [(P)Fe(C_6H_5)]^+ + e^- \quad (2)$$

$$[(P)Fe(C_6H_5)]^+ \rightleftarrows [(P)Fe(C_6H_5)]^{2+} + e^- \quad (3)$$

reduction (labeled reaction 1 in Figure 1) occurs at $E_{1/2} = -0.93$ V for (OEP)Fe(C_6H_5) and -0.70 V for (TPP)Fe(C_6H_5). This reduction is characterized by peak potential differences ($E_{pa} - E_{pc}$) of 70–80 mV at slow scan rates and peak current ratios $i_{pa}/i_{pc} = 1.0$. Investigation of this reduction at a rotating Pt disk electrode indicates Levich behavior with the maximum current proportional to $\omega^{1/2}$ in the range of rotation rates from 100 to 5800 rpm. These observations suggest a diffusion-controlled reversible to quasi-reversible one-electron transfer. The Fe(III)/Fe(II) reduction potentials for (OEP)Fe(C_6H_5) and (TPP)Fe(C_6H_5) are shifted cathodically by over 0.8 V from those of (OEP)$FeClO_4$[30] and (TPP)$FeClO_4$.[31] These potential shifts are due to the increased electron density on the metal center of (P)Fe(C_6H_5) which produces a more difficult reduction.

Attempts were made to spectrally characterize the products of reactions 1–3. The reversibility of the reduction (reaction 1) was confirmed for both (OEP)Fe(C_6H_5) and (TPP)Fe(C_6H_5) as the original spectrum was regenerated upon reoxidation. Time-resolved spectra recorded during electroreduction at controlled potential are shown in Figure 2. Both [(OEP)Fe(C_6H_5)]$^-$ and [(TPP)Fe(C_6H_5)]$^-$ were stable at the thin-layer electrode and did not exhibit any evidence of decomposition for times exceeding 10 min. The wavelengths of maximum absorbance (λ_{max}) and corresponding molar extinction coefficients (ϵ) of the generated [(P)Fe(C_6H_5)]$^-$ are shown in Table I and have spectral characteristics surprisingly close to those reported[23] for [(C_{12}TPP)Fe(n-C_4H_9)]$^-$, where C_{12}TPP represents the cross trans-linked basket-handle porphyrin.[32,33]

Upon reduction of the neutral Fe(III) complex, the Soret band is split into two bands. These occur at 350 and 408 nm for [(OEP)Fe(C_6H_5)]$^-$ and at 364 and 429 nm for [(TPP)Fe(C_6H_5)]$^-$. Isosbestic points are observed for both transitions, indicating only two species are present in solution. Lexa et al.[23] have assigned the reduction of (C_{12}TPP)Fe(n-C_4H_9) as occurring at the Fe(III) center to yield a formal Fe(II) complex. As seen in Figure 2, [(OEP)Fe(C_6H_5)]$^-$ and [(TPP)Fe(C_6H_5)]$^-$ have an absorption maximum close to 760 nm. Such an absorption band occurs for a number of anion radicals[34] and for some iron(II) and iron(III) neutral synthetic porphyrins.[35] This absorption has also been observed in the electronic absorption spectra of oxyheme complexes.[36] In the former case a porphyrin → metal charge transfer occurs, while for the latter, a d → d transition has been proposed. Finally, an $a_{2u} \rightarrow (d\pi,0\pi^*)$ transition has been calculated[36] for

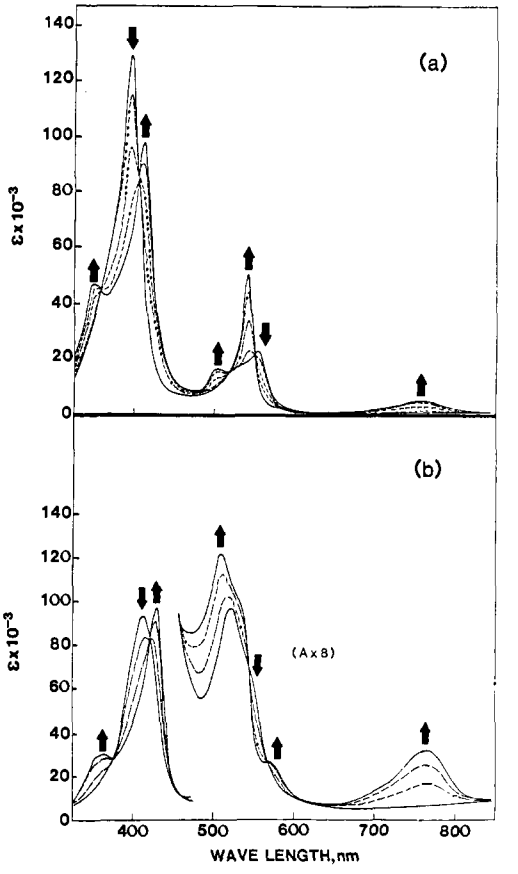

Figure 2. Time-resolved electronic absorption spectra taken at an OTTLE during the reduction of (a) 8.1×10^{-4} M (OEP)Fe(C_6H_5) and (b) 1.0×10^{-3} M (TPP)Fe(C_6H_5), in PhCN, 0.3 M TBA(PF_6). Initial and final species are represented by solid lines, while the intermediate spectra by dotted lines. Total time of electrolysis: (a) 0, 10, 20, 30, and 60 s; (b) 0, 10, 25, and 60 s.

the oxyheme derivative. For the specific case of [(P)Fe(C_6H_5)]$^-$, this assignment is not clear-cut, however, since the spectrum of the Soret region is also characteristic of an Fe(II) porphyrin, thus implying an Fe(III)/Fe(II) reaction. Because of these dual spectral properties we suggest that the electron transfer actually occurs at both sites and that the metal center is not reduced by a full unit (i.e., from Fe(III) to Fe(II)) but to an intermediate degree. The remaining electron fraction is added to a porphyrin ring orbital so that two resonance forms may be written between a formal metal-centered and a formal ring-centered reduction as shown in (4).

$$(P)Fe^{III}(C_6H_5) \rightleftharpoons \begin{matrix} [(P)Fe^{II}(C_6H_5)]^- \\ \uparrow\downarrow \\ [(P)Fe^{III}(C_6H_5)]^+\cdot \end{matrix} \quad (4)$$

Electrochemically Initiated Iron-to-Nitrogen Migration. Typical cyclic voltammograms of (OEP)Fe(C_6H_5) at a Pt electrode and

(30) Lançon, D.; Kadish, K. M. *J. Am. Chem. Soc.* **1983**, *105*, 5610.
(31) Bottomley, L. A.; Kadish, K. M. *Inorg. Chem.* **1981**, *20*, 1348.
(32) Momenteau, M.; Loock, B.; Mispelter, J.; Bisagni, E. *Nouv. J. Chim.* **1979**, *3*, 77.
(33) Momenteau, M.; Loock, B. *J. Mol. Catal.* **1980**, *7*, 315.
(34) Fuhrhop, J.-H. In "Structure and Bonding"; Springer-Verlag: New York, 1974; Vol. 18, Chapter 1.
(35) Gouterman, M. In "The Porphyrins"; Dolphin, D., Ed.; Academic Press: New York, 1978; Vol. III, Chapter I, and references therein.
(36) Loew, G. H. In "Iron Porphyrins"; Lever, A. B. P., Gray, H. B., Eds.; Addison-Wesley: Reading, MA, 1983; Part I, Chapter 1.

Table II. Maximum Absorbance Wavelengths (λ_{max}) and Corresponding Molar Absorptivities (ϵ) of *N*-Alkyl(aryl)porphyrins

species	solvent	λ_{max}, nm ($\epsilon \times 10^{-3}$)		ref
$[(N\text{-}C_6H_5OEP)Fe^{II}]^+$	PhCN[a]	395 (sh), 434 (92), 450 (sh)	544 (11), 597 (11)	this work
$[(N\text{-}C_6H_5OEP)Fe^{III}]^{2+}$	PhCN[a]	383 (82)	545 (9), 604 (10)	this work
$[(N\text{-}CH_3OEP)Fe^{III}Cl]^+ClO_4^-$	$CHCl_3$	388 (93)	504 (7), 566 (5), 661 (sh)	39
$[(N\text{-}C_6H_5TPP)Fe^{II}]^+$	PhCN[a]	453 (89), 465 (sh)	568 (6), 631 (9), 682 (6)	this work
$[(N\text{-}C_6H_5TPP)Fe^{II}]^+Cl^-$	CH_2Cl_2[b]	454 (92), 466 (sh)	569 (7), 630 (10), 682 (7)	this work
$[(N\text{-}C_6H_5TPP)Fe^{III}]^{2+}$	PhCN[a]	375 (sh), 432 (56)	570 (sh), 662 (6), 697 (6)	this work

[a] Species electrogenerated by oxidation of the corresponding (P)Fe(C_6H_5) in PhCN, 0.3 M TBA(PF_6). [b] Genuine sample; see ref 43.

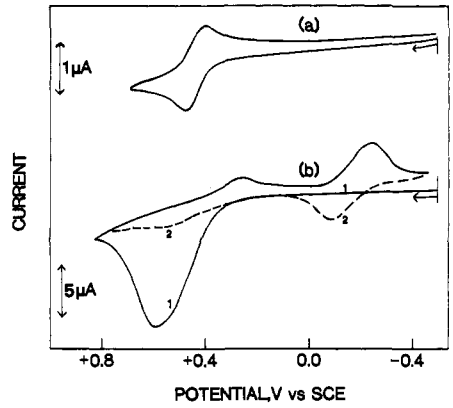

Figure 3. Cyclic voltammograms of 8.0×10^{-4} M (OEP)Fe(C_6H_5) in PhCN, 0.3 M TBA(PF_6), at (a) a Pt disk electrode, scan rate = 100 mV/s, and (b) a thin-layer gold electrode, scan rate = 3 mV/s.

at an optically transparent thin-layer gold electrode are shown in Figure 3. At scan rates >0.10 V/s, a well-defined one-electron oxidation is observed ($E_{1/2}$ = 0.48 V, Figure 3a). Values of ($E_{pa} - E_{pc}$) were equal to 60–80 mV (depending on scan rate) and $i_p/v^{1/2}$ was constant, suggesting a diffusion-controlled process.[37] However, as the scan rate was decreased below 0.10 V/s, values of $i_{pa}/v^{1/2}$ (and the related current function χ_p) increased to values greater than that expected for a one-electron transfer.[37] At the same time, the reverse cathodic peak current decreased in magnitude, suggesting an ECE mechanism. This ECE mechanism (electrochemical step followed by the chemical conversion to another electroactive species which undergoes a second electrochemical step[38]) is especially evident by the thin-layer cyclic voltammogram shown in Figure 3b. At a scan rate of 0.003 V/s the oxidation peak current is approximately double that of a one-electron transfer, while the reverse reduction peak current is almost zero. At the same time a new reversible couple is generated which has an $E_{1/2}$ of −0.18 V and a peak separation consistent with a reversible one-electron transfer.

The initial one-electron oxidation product of (OEP)Fe(C_6H_5) and the species to which it chemically converts before addition of a second electron were monitored by thin-layer spectroelectrochemistry (Figure 4a). Before electrolysis the well-characterized spectrum[26b] of (OEP)Fe(C_6H_5) (**1**) was obtained. Upon application of +0.8 V this spectrum converted to that of $[$(OEP)Fe(C_6H_5)$]^+$ (**2**). The spectrum of **2** was produced in the first 10 s of electrolysis. When the potential at +0.8 V was maintained for 7 min this spectrum slowly changed, initially producing a transient intermediate, **3**, followed by a stable species, **4**. The final product, **4**, involved a two-electron abstraction (as verified by thin-layer coulometry) and was characterized by a broadened blue-shifted Soret band (383 nm) and two absorbances at 545 and 604 nm. A similar spectrum has been reported by Ogoshi et al.[39] for $[(N\text{-}CH_3OEP)Fe^{III}Cl]^+ClO_4^-$ (see Table II) and suggests that migration of the phenyl group from the iron atom of (OEP)Fe(C_6H_5) to the nitrogen of the porphyrin ring has occurred during controlled-potential electrooxidation.

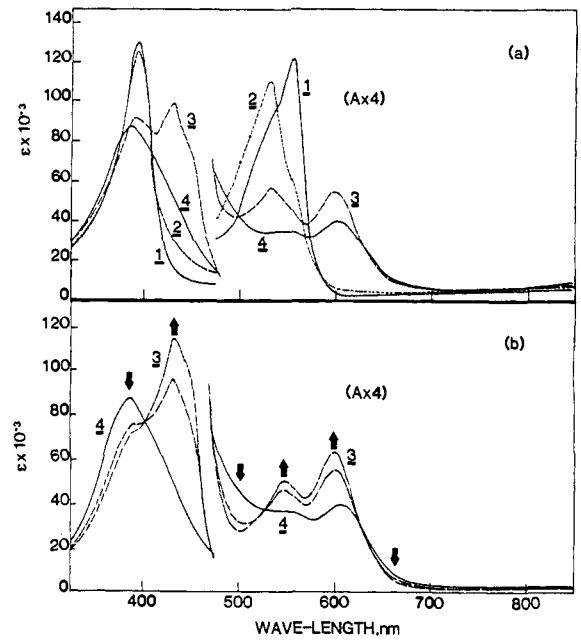

Figure 4. Time-resolved electronic absorption spectra (a) during oxidation of (OEP)Fe(C_6H_5) at +0.80 V, carried out at a thin-layer gold electrode in PhCN, 0.3 M TBA(PF_6). Time of electrolysis: 0.0 s (1), 10 s (2), 60 s (3), and 420 s (4). (b) During reduction of $[(N\text{-}C_6H_5OEP)Fe^{III}]^{2+}$, **4**, at −0.40 V, in PhCN, 0.3 M TBA(PF_6). Time of electrolysis: 0.0, 40, and 60 s.

Scheme I

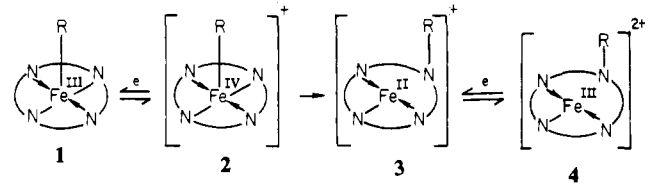

The reversible conversion of **4** to **3** after electrooxidation was easily accomplished by controlled-potential reduction at −0.4 V. This is shown in Figure 4b. The final spectrum of **3** is characterized by bands at 395 (sh), 434, 450 (sh), 544, and 597 nm (see Table II) and is similar to the spectrum reported by Lavallee[40] for the chloro(*N*-methylprotoporphyrin IX dimethyl ester)iron(II).

Analysis of the current–voltage curves and spectral analysis of the generated species suggest the electron-transfer mechanism shown in Scheme I. The overall two-electron oxidation of **1** to **4** proceeds via species **2** and **3**. Conversion of **3** to **4** is electrochemically reversible as evidenced by the reversible redox couple at −0.18 V and the presence of isobestic points on applying a potential of −0.4 V (Figure 4b).

A similar ECE mechanism is also observed for the oxidation of (TPP)Fe(C_6H_5). However, in this case the intervening chemical reaction is much faster than for the OEP derivative and the spectrum of $[$(TPP)Fe(C_6H_5)$]^+$ cannot be obtained. The final spectrum of the overall two-electron oxidation is characterized by a broadened red-shifted Soret band (432 nm) and absorbances

(37) Nicholson, R. S.; Shain, I. *Anal. Chem.* **1964**, *36*, 706.
(38) Nicholson, R. S.; Shain, I. *Anal. Chem.* **1965**, *37*, 178.
(39) Ogoshi, H.; Kitamura, S.; Toi, H.; Aoyama, Y. *Chem. Lett.* **1982**, 495.
(40) Lavallee, D. K. *J. Inorg. Biochem.* **1982**, *16*, 135.

Table III. Half-Wave Potentials for Oxidation and Reduction of Selected σ-Bonded Aryl Porphyrins and N-Alkyl(aryl)porphyrins

compd	solvent	$E_{1/2}$, V vs. SCE Fe(IV)rad/Fe(IV)	Fe(IV)/Fe(III)	Fe(III)/Fe(II)	Fe(II)/Fe(I)[g]	ref
(OEP)Fe(C_6H_5)	PhCN	1.30	0.48	−0.93		this work
	CH_2Cl_2	1.31	0.40	−0.91		this work
(TPP)Fe(C_6H_5)	PhCN	1.43[a]	0.61	−0.70		this work
	CH_2Cl_2		0.57	−0.76		this work
	DME[b]	1.52	0.67	−0.78		this work
[(*N*-C_6H_5OEP)Fe^{III}]$^{2+}$	PhCN[c]			−0.18	−1.25[d]	this work
[(*N*-C_6H_5TPP)Fe^{III}]$^{2+}$	PhCN[c]			−0.06	−0.97[d]	this work
[(*N*-CH_3TPP)Fe^{II}]$^{+}Cl^-$	CH_2Cl_2[e]			+0.49	−0.90	41
[(*N*-CH_3PPDME)Fe^{II}]$^{+}Cl^-$	CH_3CN[f]			+0.355	−1.02	40

[a] Potential quoted is E_{pa} at 0.01 V/s. [b] Potentials quoted are $E_{1/2}$ measured at −50 °C. [c] [(*N*-C_6H_5P)Fe^{III}]$^{2+}$ was electrogenerated at a thin-layer electrode, in PhCN, 0.3 M TBA(PF_6). Applied potential: +0.80 V (P = OEP); +1.00 V (P = TPP). [d] Potential quoted is E_{pc}, measured at 3 mV/s, at a thin-layer electrode. [e] In CH_2Cl_2, 0.1 M TBA(ClO_4). [f] In CH_3CN, 0.1 M TBA(ClO_4). [g] The electrode reaction gives a product formally existing as iron(I). The actual product may be an iron(II) anion radical.

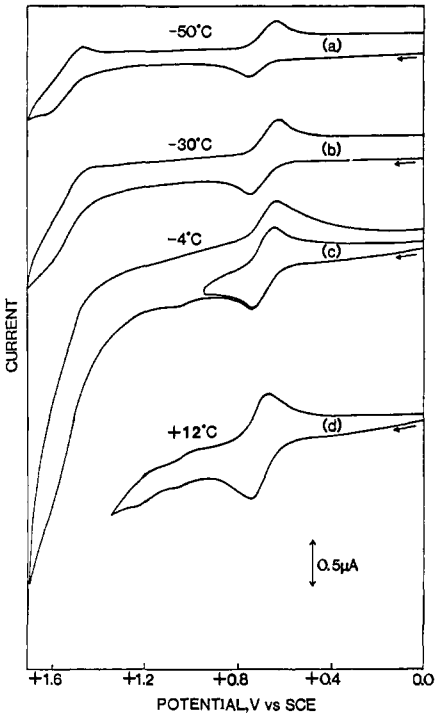

Figure 5. Temperature-resolved cyclic voltammograms of 1.0×10^{-3} M (TPP)Fe(C_6H_5) in DME, 0.1 M TBA(PF_6). Scan rate = 100 mV/s. Temperature: (a) −50 °C; (b) −30 °C; (c) −4 °C; (d) +12 °C.

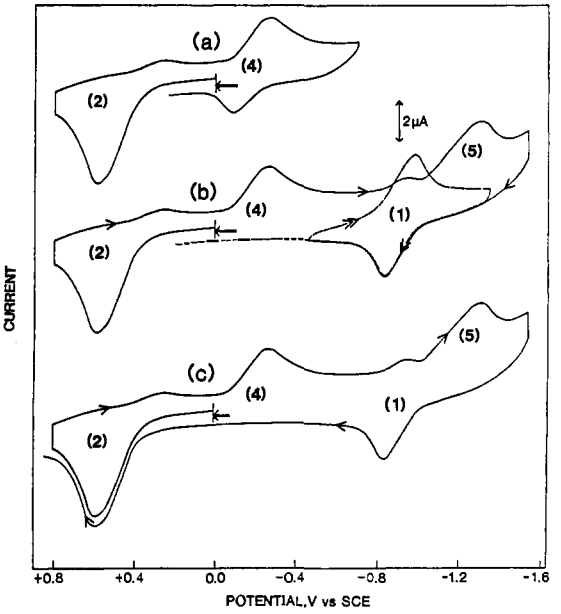

Figure 6. Cyclic voltammograms of 6.0×10^{-4} M (OEP)Fe(C_6H_5) in PhCN, 0.3 M TBA(PF_6), carried out at a thin-layer gold electrode. Scan rate = 3 mV/s.

at 570, 662, and 697 nm. Like the OEP derivative this species can be reversibly reduced by one electron (at $E_{1/2}$ = +0.06 V) to yield a stable product with an electronic absorption spectrum of (*N*-C_6H_5TPP)Fe^{II}Cl. This latter complex can also be obtained by oxidation of (TPP)Fe^{III}(C_6H_5) by $FeCl_3$.[19]

As expected, both complexes **3** and **4** are air-stable. The observed half-wave potentials for the Fe^{III}/Fe^{II} reaction of [(*N*-C_6H_5OEP)Fe^{III}]$^{2+}$ and [(*N*-C_6H_5TPP)Fe^{III}]$^{2+}$ in PhCN are given in Table III and are cathodically shifted by 415–670 mV from values reported by Lavallee for the Fe^{III}/Fe^{II} reaction of *N*-CH_3TPP)Fe^{II}Cl in CH_2Cl_2, 0.1 M TBAP,[41] and (*N*-CH_3PPDME)Fe^{II}Cl in CH_3CN, 0.1 M TBAP.[40] These shifts may be attributed to differences in inductive effects between the CH_3 and C_6H_5 N-bound groups, as well as to differences in the solvent, the counterion, or the nature of the porphyrin ring.[42]

At fast scan rates or low temperatures, oxidation of [(P)Fe(C_6H_5)]$^+$ (reaction 3) can occur before migration of the phenyl group. This is shown in Figure 1 where the second oxidation is well defined for [(OEP)Fe(C_6H_5)], but not for [(TPP)Fe(C_6H_5)], which rapidly undergoes the ECE mechanism. Attempts were made to stabilize the electrogenerated [(TPP)Fe(C_6H_5)]$^{2+}$ species both by changing the solvent and by lowering the temperature from +23 to −50 °C. Several solvent systems were investigated, and the best reversibility was obtained in 1,2-dimethoxyethane (DME) at −50 °C. Cyclic voltammograms in this solvent are shown in Figure 5, where the initial experiments were carried out at −50 °C and the temperature then was increased to +12 °C. Attempts to go from high to low temperatures were unsuccessful due to decomposition of (TPP)Fe(C_6H_5) at room temperature in this solvent.

Scheme II

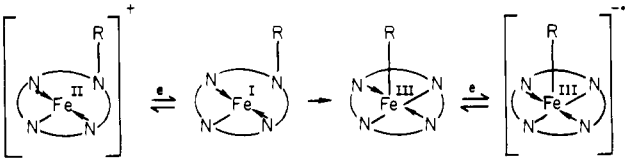

Attempts were also made to spectrally characterize the second oxidation product(s) of (P)Fe(C_6H_5). However, at the thin-layer spectroelectrochemistry time scale, the iron-to-nitrogen migration of the phenyl group occurred before [(P)Fe(C_6H_5)]$^{2+}$ could be significantly formed. In addition, demetalation of the resulting [(*N*-C_6H_5P)Fe]$^{2+}$ complexes also occurred, giving rise to the free base dication, [(*N*-C_6H_5P)H]$^{2+}$. This reaction has been described in the literature.[18,19]

(41) Anderson, O. P.; Kopelove, A. B.; Lavallee, D. K. *Inorg. Chem.* **1980**, 19, 2101.

(42) Genuine samples of (*N*-C_6H_5TPP)Fe^{II}Cl have an $E_{1/2}$ = +0.44 V for the Fe^{II}/Fe^{III} reaction in PhCN, 0.1 M TBA(PF_6), suggesting that the predominant effect on $E_{1/2}$ is the relative strength of the counterion bound to Fe(II) (in this case Cl^- vs. PF_6^-).

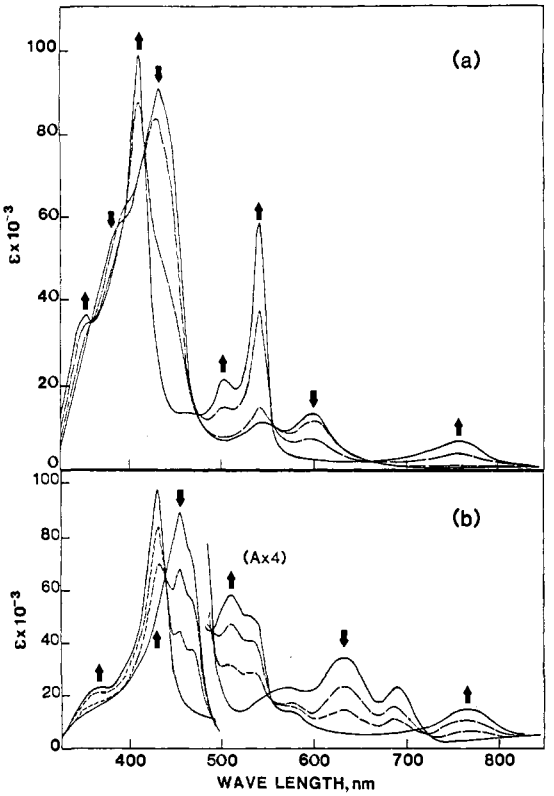

Figure 7. Reduction of electrogenerated (a) 6.0×10^{-4} M $[(N\text{-}C_6H_5OEP)Fe^{II}]^+$ and (b) 6.5×10^{-4} M $[(N\text{-}C_6H_5TPP)Fe^{II}]^+$ at the OTTLE, in PhCN, 0.3 M $TBA(PF_6)$. The applied potentials were cathodic from those presented in Table III for the reduction of $[(N\text{-}C_6H_5P)Fe]^+$.

Electrochemically Initiated Nitrogen-to-Iron Migration. The overall two-electron reduction of electrogenerated $[(N\text{-}C_6H_5OEP)Fe]^+$ to give $[(OEP)Fe(C_6H_5)]^-$ was confirmed by cyclic voltammetry (Figure 6), controlled potential electrolysis, and spectral product identification at the thin-layer gold electrode. These results suggest that a nitrogen-to-iron migration of the phenyl group in $[(N\text{-}C_6H_5OEP)Fe]^+$ also takes place by means of an ECE mechanism as outlined in Scheme II.

Monitoring of the spectral changes during the two-electron reduction of $[(N\text{-}C_6H_5P)Fe]^+$ (process 5, Figure 6) indicated a quantitative conversion to $[(P)Fe(C_6H_5)]^-$. This is shown in Figure 7 for both OEP and TPP derivatives. No isobestic point was observed during the reduction, thus suggesting the presence of intermediates along the overall two-electron addition. Furthermore, genuine samples of $[(N\text{-}C_6H_5P)Fe^{II}]Cl$[43] reduced at a thin-layer electrode under the same experimental conditions yielded the same final spectra. These observations confirm an electrochemically induced back-migration from nitrogen to iron. Finally, reversible oxidation of $[(P)Fe(C_6H_5)]^-$ at the thin-layer electrode

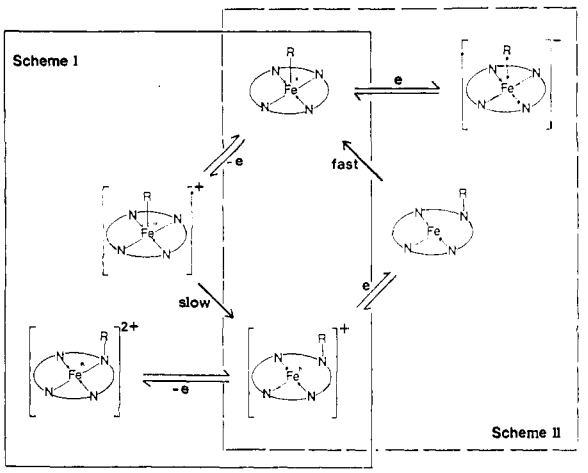

Figure 8. Schemes illustrating reversible iron-to-nitrogen migration of $(P)Fe(C_6H_5)$ and $[(N\text{-}C_6H_5P)Fe]^+$.

quantitatively yielded the initial $(P)Fe(C_6H_5)$. This is shown by peak 1 in Figure 6b,c. The overall reversible oxidation/reduction scheme involving reversible migration of the phenyl group is shown in Figure 8.

Effect of the Iron–Carbon σ Bond and Site of the Electrode Reactions. In noncoordinating solvents, the (P)Fe(R) porphyrins where R = CH_3, n-C_4H_9, C_6H_5, or p-$CH_3C_6H_4$ are five-coordinate low-spin $S = {}^1/_2$ complexes as evidenced by their ^1H NMR characteristics.[26,44] The alkyl or aryl group acts as a strong field ligand leading to a raising of the energy levels of the iron $d_{x^2-y^2}$ and d_{z^2} orbitals. Analysis of the observed chemical shifts by NMR spectroscopy[26b,44] leads to the conclusion that metal to axial ligand charge transfers of large magnitude occur in these complexes. In addition, strong blue-shifted Q bands in the electronic absorption spectra of (P)Fe(R)[26b] are indicative of an increased electron density on the metal ion.

Although the iron is formally in the +III oxidation state in (P)Fe(R) complexes, these species behave as if they contain a "reduced" iron(II) center. The magnitude of the electron density on the metal for a given type of porphyrin (e.g., octaethyl- or tetraphenylporphyrin) is strictly dependent on the inductive effect of R.[28] This same factor dictates the relative stability of the iron–carbon σ bond in (P)Fe(R): the more electron donating the alkyl (aryl) group, the less stable the Fe–C σ bond.

In all media where $(P)Fe(C_6H_5)$ compounds are stable, the first oxidation and first reduction potentials are dramatically shifted from those of (P)FeX. For example, in PhCN, 0.1 M $TBA(PF_6)$, $(TPP)Fe(C_6H_5)$ is oxidized at +0.61 V and reduced at −0.70 V while $(TPP)FeClO_4$ is oxidized at +1.13 V and reduced at +0.20 V in the same solvent containing 0.1 M $TBA(ClO_4)$.[31] Such shifts can be explained by the increased electron density on the metal induced by the iron–carbon σ bond.

Electronic absorption spectra of the species obtained after addition of one electron strongly suggest both an iron(III) radical anion and an iron(II) formulation as depicted in eq 4. Such electron transfers have already been evoked to rationalize the electronic absorption spectra of species generated upon the two-electron reduction of (TPP)FeX.[45] In this case the contribution of a spin-coupled iron(II) radical anion to the iron(I) porphyrin formulation has been suggested.

Since the (P)Fe(R) porphyrins are low-spin $S = {}^1/_2$ iron(III) complexes, the reduction scheme outlined by eq 4 implies that the d_{xz} and d_{yz} orbitals of the d^5 iron ion and the porphyin e_g LUMO of the same symmetry may have similar overlapping energy levels. In this case, the d orbitals of the iron ion in (P)-Fe(R) must exhibit uncommonly high energy levels. As a con-

(43) Analytical samples of $(N\text{-}C_6H_5P)Fe^{II}Cl$ were prepared by electroinduced oxidative migration from metal to nitrogen in $(P)Fe(C_6H_5)$ followed by demetalation, purification of the N-phenylporphyrin obtained, and metalation using $FeCl_2$ in THF.[41] A typical experiment is described as follows: Two 10-mg samples of $(P)Fe(C_6H_5)$ in CH_2Cl_2, 0.1 M $TBA(PF_6)$, were electrolyzed at +0.8 V (OEP) or +1.0 V (TPP). The $[(N\text{-}C_6H_5P)Fe^{III}]^{2+}$ complexes so obtained were demetalated by addition of dilute hydrochloric acid, washed with water containing small amounts of collidine or aqueous NH_4OH, and dried over sodium sulfate. The solvent was then evaporated under reduced pressure. The supporting electrolyte was removed by dissolving the crude material in a few milliliters of methanol or diethyl ether, cooling the solution, and filtrating rapidly by suction on a medium frit. The procedure was repeated four times. After evaporation of the solvent and redissolution of the solid in methylene chloride, the products obtained exhibited absorbances characteristic of $(N\text{-}C_6H_5TPP)H$ (444, 550 (sh), 595, 633 (sh), and 705 nm)[18] and $(N\text{-}C_6H_5OEP)H$ (420, 520, 544, 603, and 657 nm). Treatment of the above N-phenylporphyrins with anhydrous $FeCl_2$ dissolved in boiling oxygen-free THF gave the $(N\text{-}C_6H_5P)Fe^{II}Cl$ derivatives, which were identified by their electronic absorption spectra.[39-41]

(44) Lançon, D.; Cocolios, P.; Guilard, R.; Kadish, K. M. *Organometallics* **1984**, *3*, 1164–1170.

(45) Reed, C. A. In "Electrochemical and Spectrochemical Studies of Biological Redox Components"; Kadish, K. M.; Ed.; American Chemical Society: Washington, DC, 1982; Adv. Chem. Ser. No. 201, p 333.

sequence, the energy for ionization of the iron ion in these complexes is dramatically lowered, thus rendering more accessible the iron(IV) oxidation state. The d-orbital energy levels must be directly related to the inductive effect of the axial σ-bonded group. This assumption is strengthened by the fact that half-wave potentials of +0.25 and +0.39 V are observed for (OEP)Fe(n-C_4H_9) and (C_{12}TPP)Fe(n-C_4H_9), respectively,[23] compared to potentials of +0.48 V for oxidation of (OEP)Fe(C_6H_5) and +0.61 V for oxidation of (TPP)Fe(C_6H_5).

The half-wave potential of the second oxidation appears to be insensitive to the nature of the axial ligand. This electron transfer takes place at E_{pa} = +1.43 V in CH_2Cl_2 or $E_{1/2}$ = +1.52 V in DME, 0.1 M TBA(PF_6), for (TPP)Fe(C_6H_5) while the oxidation half-wave potential for (TPP)FeX occurs at $E_{1/2}$ = +1.40 V in CH_2Cl_2, 0.1 M TBA(ClO_4) (where X stands for an anionic halide or pseudohalide).[31] These observations suggest that the first oxidation of (P)Fe(C_6H_5) effectively occurs at the metal center.

The electronic absorption spectra of the one-electron oxidized species obtained are in agreement with the above statement. For example, [(OEP)Fe(C_6H_5)]$^+$ does not exhibit any absorption band above 600 nm (see Table I and Figure 4a). In addition, the Soret band wavelength and molar extinction coefficients are very close to the corresponding values of the neutral complex, indicating that the removal of one electron from (OEP)Fe(C_6H_5) does not affect the π system of the porphyrin. Furthermore, a sharp blue-shifted β band is observed in the spectrum. This absorbance is not found in any reported cation radical electronic absorption spectrum in the porphyrinic series. Consequently, one may describe these one-electron oxidized species as [(P)Fe^{IV}(C_6H_5)]$^+$.

Acknowledgment. The support of the National Institutes of Health (GM 25172) is gratefully acknowledged.

Registry No. (OEP)Fe(C_6H_5), 83614-06-6; [(OEP)Fe(C_6H_5)]$^+$, 90790-40-2; [(OEP)Fe(C_6H_5)]$^-$, 90790-41-3; (TPP)Fe(C_6H_5), 70936-44-6; [(TPP)Fe(C_6H_5)]$^-$, 90790-42-4; [(N-C_6H_5OEP)Fe^{II}]$^+$, 90790-43-5; [(N-C_6H_5OEP)Fe^{III}]$^{2+}$, 90790-44-6; [(N-C_6H_5TPP)Fe^{II}]$^+$, 90790-45-7; [(N-C_6H_5TPP)Fe^{II}]$^+Cl^-$, 83219-61-8; [(N-C_6H_5TPP)Fe^{III}]$^{2+}$, 90790-46-8.

Unusual Bond Lengths, Conformations, and Ligand Exchange Rates in B_{12} Models with the Bis(salicylidene)-*o*-phenylenediamine Equatorial Ligand

Michael F. Summers,[†] Luigi G. Marzilli,*[†] Nevenka Bresciani-Pahor,[‡] and Lucio Randaccio*[‡]

Contribution from the Department of Chemistry, Emory University, Atlanta, Georgia 30322, and Istituto di Chimica, Universita di Trieste, 34127, Trieste, Italy. *Received October 11, 1983*

Abstract: Convenient synthetic procedures for B_{12} models containing saloph (dianion of bis(salicylidene)-*o*-phenylenediamine) are reported. The crystal and molecular structure of two compounds containing pyridine (py) in one axial position are described. Compound I, ((py)Co^{III}(saloph)C_2H_5)·H_2O, ($C_{27}H_{24}CoN_3O_2$·H_2O), crystallizes in space group $P2_1/c$ with a = 12.140 (7) Å, b = 12.736 (8) Å, c = 15.822 (9) Å, β = 100.2 (1)°, V = 2407.7 Å^3, D_{measd} = 1.37 (1) g cm^{-3}, D_{calcd} = 1.38 g cm^{-3}, and Z = 4. A total of 6319 reflections were measured. Compound II, ((py)Co^{III}(saloph)CH_2CN)·H_2O, ($C_{27}H_{21}CoN_4O_2$·H_2O), crystallizes in space group $P2_1/n$ with a = 13.964 (7) Å, b = 12.219 (7) Å, c = 14.903 (8) Å, β = 110.6 (1)°, V = 2380.3 Å^3, D_{measd} = 1.42 (1) g cm^{-3}, D_{calcd} = 1.43 g cm^{-3}, and Z = 4. A total of 7532 reflections were measured. The structures were solved with conventional Patterson and Fourier methods. Block-diagonal least-squares refinement led to final R values of 0.035 and 0.049 for I and II, respectively. The most unusual structural feature in these compounds is the orientation of the py ligand of I in that it is positioned over the five-membered chelate ring made by the phenylenediamine moiety. This orientation has not been observed previously. The reason for this unusual orientation is discussed in terms of the very long Co–N(py) bond in I of 2.215 (4) Å, which is the longest bond found to date in any B_{12} model. In II, this bond is shorter, 2.098 (4) Å, reflecting the weaker trans influence of CH_2CN compared to C_2H_5. The py lies over the six-membered chelate rings (the normal situation). The bond lengths and bond angles at the alkyl moiety are typical. However, the saloph moieties are distinctly nonplanar with the two salicylaldiminato units forming dihedral angles of −25.4 and 17.7° in I and II, respectively. Thus the distortions are in opposite directions. This difference can also be understood in terms of the Co–N bond lengths. These bond lengths are ~0.1 Å longer than those found with comparable axial ligand sets in cobaloximes, where the equatorial ligand system comprises two dioximato ligands. Dynamic NMR methods allowed estimates of ligand exchange rates at 25 °C for compounds similar to II but with 3,5-lutidine (3,5-LUT). Two types of comparison were made. From reasonable estimates of exchange rates for the cobaloximes with the 3,5-LUT/CH_2CN ligand set, the reactivity of the saloph compound with these axial ligands is 10^{10} times as large. It is argued that this enormous cis influence is partly a ground-state effect and partly arises from the higher stability of saloph five-coordinate intermediates compared to cobaloxime five-coordinate intermediates. For example, the cobaloxime with the py/i-C_3H_7 axial ligand set has a Co–N bond length very similar to that of II. Yet the ligand exchange rate of the cobaloxime is estimated to be 10^4 times less than that in II. The relevance of these findings to estimated Co–C bond dissociation energies (BDE) in models and to the Co–C bond homolysis reaction in B_{12}-dependent processes is discussed.

Introduction

Catalytic processes involving B_{12}-dependent enzymes are complex.[1] Proposed components of the mechanisms include formation of the holoenzyme–substrate complex (accompanied by conformational changes in both the enzyme and B_{12} coenzyme), homolytic cleavage of the Co–C bond, H atom abstraction from the substrate by the deoxyadenosyl radical formed by homolysis, substrate rearrangement to product (either via a radical pathway

[†] Emory University.
[‡] Universita di Trieste.

(1) "B_{12}"; Dolphin, D., Ed.; Wiley-Interscience: New York, 1982.

0002-7863/84/1506-4478$01.50/0